



[haematologica]
2004;89:330-337

NÚRIA PUJOL-MOIX
MICHAEL J KELLEY
ANGEL HERNÁNDEZ
EDUARDO MUÑOZ-DÍAZ
IGNACIO ESPAÑOL

Ultrastructural analysis of granulocyte inclusions in genetically confirmed MYH9-related disorders

A B S T R A C T

Background and Objectives. MYH9-related disorders are autosomal dominant hereditary macrothrombocytopenias caused by mutations in the *MYH9* gene. This gene encodes the non-muscular myosin heavy chain type II A (MHCIIA). Among these disorders, May-Hegglin anomaly (MHA), Sebastian syndrome (SS), and Fechtner syndrome (FS) are associated with different types of ribosome inclusions in granulocytes. FS also exhibits Alport-like manifestations: nephropathy, neurosensory deafness, and cataracts. The aim of our study was to assess the granulocyte inclusion ultrastructure in genetically confirmed MYH9-related disorders.

Design and Methods. Ten individuals were studied. All fulfilled the clinical and laboratory findings to be diagnosed as having an MYH9-related disorder. The ultrastructure of 50 granulocyte sections for each patient was examined, and the percentages of the different types of inclusion were established. Mutations of the *MYH9* gene were also analyzed.

Results. The patients were classified as having MHA if the inclusions contained parallel longitudinal filaments. If not, they were classified as having SS or FS. FS patients also showed Alport-like manifestations. In all syndromes we observed a wide variability of the inclusion ultrastructure. Moreover, a small number of inclusions typical of other syndromes was observed. A new cross-striated inclusion variant was identified in SS. A significant number of pure ribosome aggregates were identified in all syndromes.

Interpretation and Conclusions. Like other MYH9-related traits, the variation and partial overlap in the inclusion ultrastructure could be attributed to specific changes in the polymerization, assembly, or stability of the MHCIIA. These changes might be associated with *MYH9* gene mutations as well as with its heterogeneous expression.

Key words: MYH9-related disorders, May-Hegglin anomaly, Fechtner syndrome, Sebastian syndrome, granulocyte inclusions.

From the Departament d'Hematologia, Hospital de la Santa Creu i Sant Pau, Barcelona, Spain (NP-M, AH, EM-D); Departament de Medicina, Universitat Autònoma de Barcelona, Spain (NP-M, IE); Department of Medicine, Duke University Medical Center and Durham Veterans Affairs Hospital, Durham, NC, USA (MJK).

Correspondence: Dr. Núria Pujol-Moix, MD, Hospital de la Santa Creu i Sant Pau Departament d'Hematologia Sant Antoni M. Claret, 167 08025-Barcelona, Spain E-mail: npujol@hsp.santpau.es

©2004, Ferrata Storti Foundation

MYH9-related disorders are a group of autosomal dominant hereditary macrothrombocytopenias characterized by few hemorrhagic manifestations, large platelets in blood smears, and, in the majority of cases, Döhle-like inclusions in granulocytes. This association was reported for the first time by May¹ and Hegglin.² The granulocyte inclusions in the May-Hegglin anomaly (MHA) appear as blue-grayish spots under light microscopy (Figure 1). They are pyroninophilic using methyl-green-pyronin staining, indicating their RNA nature.³ The same syndrome has also been reported in one family whose members additionally suffered clinical manifestations of nephropathy, high tone neurosensory deafness, and cataracts resembling Alport syndrome.^{4,5} The inclusions of this disorder -the Fechtner syndrome (FS)- were less prominent than those observed in MHA. Identical inclusion mor-

phology was subsequently demonstrated in a family with macrothrombocytopenia but without Alport features: the Sebastian syndrome (SS).^{6,7}

At the ultrastructural level, all inclusions are partially limited by short strands of rough endoplasmic reticulum (RER) filled with ribosomes,^{4,6} and, in the MHA type, also show fine electron-dense filaments organized along the long axis of the inclusion (Figures 2A, 2B, 3A). A distinct inclusion type has been identified in one FS family:⁸ this is elongated spindle-shaped inclusion body filled with clusters of ribosomes arranged in a banded, cross-striated organization (Figure 4A). Another type of inclusion has recently been reported in SS:⁹ this is mainly elongated, membrane-free, and filled with ribosomes. Some inclusions reveal a sharp bend in the rod, like the letter L, or are relatively spherical. These inclu-

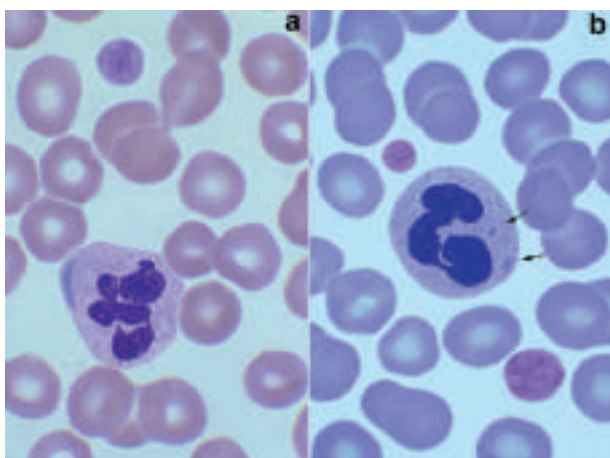


Figure 1. Granulocyte inclusions: light microscopy. Air-dried blood films stained with May-Grünwald-Giemsa ($\times 1000$) showing: a) one giant platelet, and one neutrophil granulocyte with a bright blue spindle-shaped inclusion (near the cell membrane) typical of the May-Hegglin anomaly; b) two giant platelets, and one neutrophil granulocyte with two faint-blue irregularly-shaped inclusions (arrows), typical of the Sebastian and Fechtner syndromes.

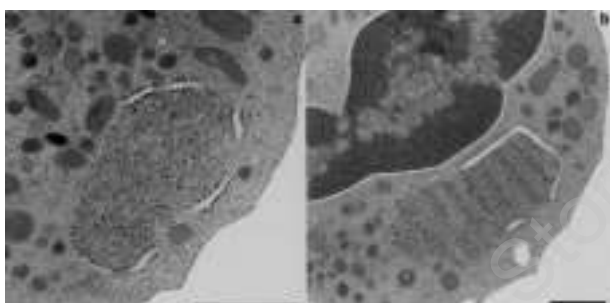


Figure 3. Fechtner/Sebastian inclusions. Electron micrographs of neutrophil granulocytes showing: a) the typical inclusion described in Fechtner and Sebastian syndromes composed of clusters of ribosomes, and segments of rough endoplasmic reticulum but no longitudinal filaments; b) an inclusion with a similar composition revealing a cross-striated distribution of its ribosome matrix; bars = 1 μm .

sions are segmented by fragments of smooth endoplasmic reticulum (SER) together with glycogen particles, which give a cross-striated appearance.

Genetic studies have demonstrated that all of these syndromes are associated with mutations in the *MYH9* gene located in chromosome 22q11.2, which encodes non-muscle myosin heavy chain IIA (MHCIIA).¹⁰ Even in the Epstein syndrome, which has most features of FS but lacks granulocyte inclusions, mutations in the same gene have been detected.¹¹ All of these findings suggest that different types of mutations in *MYH9* gene result in the distinct phenotypic syndromes, which are allelic variants. Accordingly, it has recently been proposed that this group of diseases be defined

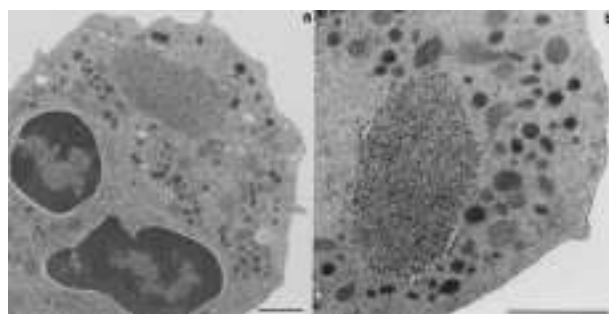


Figure 2. May-Hegglin inclusions. Electron micrographs of neutrophil granulocytes showing: a) a cell with normal morphology, except for one cytoplasmic inclusion body; b) an inclusion composed of clusters of ribosomes, segments of rough endoplasmic reticulum and electron-dense filaments oriented along the long axis of the inclusion; bars = 1 μm .

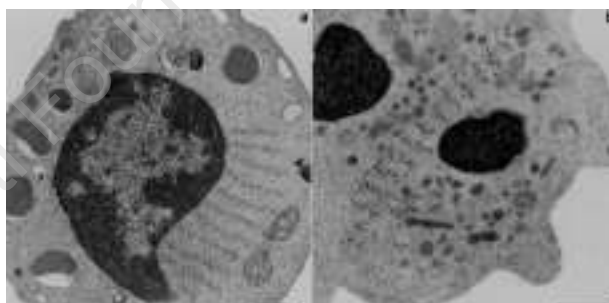


Figure 4. Fechtner inclusions. Electron micrographs of a basophil and a neutrophil granulocyte, each showing elongated inclusions composed of clusters of ribosomes, in a banded cross-striated organization without any filaments; a) in the basophil, the inclusion is located in the perinuclear area and the bands are oriented radially; b) in the neutrophil the inclusion is much more elongated and covers a larger area of the cytoplasm; bars = 1 μm .

as *MYH9-related disorders*¹² or *MHCIIA syndromes*.¹³ In contrast, the true Alport syndrome is caused by mutations in the α chain of type IV collagen genes located on chromosomes X, 2, and 13.¹⁴

The human non-muscular myosins, type A and type B, are widely co-expressed in tissues but some tissue sites have differential expression.¹⁵ MHCIIA is preferentially expressed in the cochlea and kidney, and is the exclusive myosin heavy chain in granulocytes and platelets. This may explain the limited pathology observed when MHCIIA is genetically abnormal, and also the predominance of granulocyte and platelet anomalies.

In our previous experience with hereditary macrothrombocytopenias with granulocyte inclusions, we

Table 1. MYH9-related disorders with granulocyte inclusions: general data, gene mutations, and light microscopy results.

Diagnosis	Family Case	Familial relationship	Age Sex	MYH9 gene mutations	*Platelet counts ($\times 10^9/L$)		°Giant platelets (%)	Fraction of granulocytes with inclusions (%)	Predominant inclusion type
					Electronic	Microscopic			
MHA	A1	Proband	53 F	E1841K exon 38	35	80	62	92	Bright blue spindle-shaped
MHA	A2	Mother	78 F	nd	75	130	25	98	Bright blue spindle-shaped
SS	B3	Proband	30 F	R1933X exon 40	13	90	21	69	Faint blue irregular-shaped
SS	B4	Mother	55 F	R1933X exon 40	40	94	7	61	Faint blue irregular-shaped
SS	C5	Proband	38 F	R1933X exon 40	35	87	12	74	Faint blue irregular-shaped
SS	C6	Son	12 M	R1933X exon 40	24	93	31	69	Faint blue irregular-shaped
FS	D7	Proband	70 F	R1165C exon 26	75	154	15	46	Faint blue irregular-shaped
FS	D8	Daughter	33 F	R1165C exon 26	68	85	15	47	Faint blue irregular-shaped
FS	D9	Daughter	44 F	R1165C exon 26	81	153	13	67	Faint blue irregular-shaped
FS	E10	Proband	58 M	D1424Y exon 30	16	60	53	95	Faint blue irregular-shaped

*Platelet counts (normal range is 150 to 350); °Giant platelets: platelets of 4.0 μm or more in diameter (non-anticoagulated blood films); nd: not determined; MHA: May-Hegglin anomaly; SS: Sebastian syndrome; FS: Fechtner syndrome.

noted that inclusion numbers and ultrastructural morphology vary greatly among different members of the same family and over time in the same individual. Moreover, mixed types of inclusions could be observed in different cells of the same sample, and even in the same cell.

The aim of the present study was to assess the granulocyte inclusion characteristics in 10 cases of genetically confirmed MYH9-related disorders. This assessment included numerical evaluation of the granulocyte inclusions, the proportion of the classic and new types of inclusions and, in a selected group of patients, their variations during a two-year follow-up.

Design and Methods

Ten individuals from 5 unrelated families were enrolled in the study (Table 1). Some aspects of family D have been previously reported.^{8,16} Informed consent to this study was obtained from all the participants according to the Declaration of Helsinki. The diagnosis of an MYH9-disorder was based on clinical and laboratory findings including granulocyte ultrastructure and genetic studies. A full clinical evaluation was done in all

individuals and included assessment of bleeding, kidney function, hearing and sight. In addition to standard blood and biochemistry tests, a phase microscopy platelet count,¹⁷ and a careful examination of granulocytes and platelets by light microscopy were performed. Moreover, a granulocyte ultrastructural study and mutational analysis of the MYH9 gene were carried out. In 5 patients (A1, B4, C5, D7, D9), a second evaluation was made approximately two years later.

Light microscopy

Air-dried blood films, obtained without anticoagulant, were stained with panoptic May-Grünwald-Giemsa buffered at pH 7.8, within 3 hours of withdrawal. Using an immersion oil objective, 100 granulocytes were examined and the percentage of these containing inclusions was determined. Size, shape and clarity of the inclusions, as well as their number per cell and the granulocyte classes containing them were evaluated. The general morphology of platelets and red blood cells was examined and platelet size measured on the same non-anticoagulated blood smear. Platelets measuring 4.0 μm or more in diameter are considered as giant. Blood films were also stained with methyl-green-pyronin⁶ and periodic acid Schiff (PAS).¹⁸

Granulocyte ultrastructure

For granulocyte ultrastructure examinations, the samples were obtained and processed as previously described.¹⁹ Briefly, buffy coats of citrated blood were fixed with 1.5 % glutaraldehyde in 0.1 M cacodylate buffer at pH 7.3. Specimens were then postfixed in 1 % osmium tetroxide in the same buffer, dehydrated in graded series of ethanol, and embedded in Epon 812 following standard methods. The ultrathin sections were stained with uranyl acetate and lead citrate and were observed, in a blinded fashion, in a Hitachi 600 AB transmission electron microscope with an accelerating voltage of 80 KV. Apart from examining the general cellular traits, a careful analysis of the inclusions was carried out in granulocyte electron micrographs. Beside its size and shape, the structures contained in the inclusion (RER, SER, single ribosomes and clusters, filaments, amorphous material) and their organization were evaluated. The percentages of the different types of inclusion were determined, based on these observations in a minimum of 50 granulocyte sections. The results were compared with those obtained in a group of 15 healthy individuals.

Genetic studies

Genetic analysis of *MYH9* was performed as previously described.²⁰ Briefly, each of the 40 coding exons of *MYH9* was amplified individually by polymerase chain reaction (PCR) from genomic DNA isolated from peripheral blood. PCR products were directly sequenced. Exons with variants were confirmed by sequencing on the opposite strand and/or by restriction fragment length polymorphism analysis.

Results

Age, sex, familial relationships, and the specific type of MYH9-related disorder of the 10 cases studied are shown in Table 1. Different degrees of thrombocytopenia were observed in the electronic counts of all individuals. Platelet counts performed by phase microscopy showed a thrombocytopenia that was much less marked; in two individuals the counts were even in the minimum normal range. Granulocyte inclusions and a family history revealing an autosomal dominant hereditary pattern were present in all cases. Some patients suffered from a mild hemorrhagic diathesis, manifested mainly as easy bruising and mucous bleeding (A1, B3, B4, C5, D7, D8, D9). No hemorrhagic manifestations were observed in the remaining cases. Following previously established diagnostic criteria,²¹ the individuals without Alport-like manifestations were classified as having MHA if their granulocyte inclusions clearly exhibited the classic filaments

along the longitudinal axis. When longitudinal filaments were absent in more than 90 % of inclusions, the patients were classified as having SS. The patients who additionally developed a progressive high tone neurosensory deafness were classified as having FS. None of our patients had other Alport-like features such as nephropathy or cataracts.

Light microscopy

The frequency of granulocyte inclusions and their characteristics, together with the percentage of giant platelets are reported in Table 1. Inclusions were seen in neutrophils, eosinophils, basophils, and monocytes, although these last cells were not included in the quantitative evaluation. Typical bright blue spindle-shaped MHA inclusions, about 2–5 µm in length, were found mainly in the MHA patients. They were generally single (occasionally two per cell) and mainly, but not exclusively, located in the periphery of the cytoplasm (Figure 1A). Faint blue irregularly shaped inclusions, about 1–2 µm in diameter, were mainly observed in the cases of SS and FS (Figure 1B). These frequently appeared singly or in pairs but sometimes, 3 or more small inclusions were seen in all areas of the cytoplasm. Although the predominant inclusion type remained constant, the number of inclusions varied over time in some patients (Table 3). The cytoplasm of granulocytes stained normally with PAS stain. However, the inclusions were PAS negative, and were thus seen as well-defined clear areas. In contrast, the inclusions were pyroninophilic with the methyl-green-pyronin staining.

Granulocyte ultrastructure

The general ultrastructural morphology of granulocytes was typically normal including nuclear chromatin and lobulation, and cytoplasmic granulation. Granulocyte inclusions were located in cytoplasmic areas devoid of granules. A single inclusion was generally present for each cell section but in some cells two or more could be detected. Apart from the classic MHA and FS/SS inclusion types and the elongated cross-striated inclusion previously described, some new inclusion types were observed (Tables 2 and 3). Although a predominant inclusion class was present in most patients, generally more than one class appeared, even in the same cell. Overall, the following granulocyte inclusions were identified.

MHA inclusions. The MHA inclusions were generally spindle-shaped bodies about 1.7 to 4.5 µm in length and 0.9 to 1.8 µm in width (Figure 2). They were not enclosed by membrane and usually showed some fragments of RER in the periphery. Single and clustered ribosomes were the main constituents of the matrix, which also contained filaments (about 7–10 nm thick). These filaments always appeared organized in parallel

Table 2. MYH9-related disorders: granulocyte inclusion ultrastructure.

Diagnosis	Family Case	MHA	*Inclusion types (%)			
			FS/SS		ECS	RA
			Classic	Cross striated		
MH	A1	58	38	0	0	4
MHA	A2	36	43	0	0	21
SS	B3	2	41	37	0	20
SS	B4	0	30	36	0	34
SS	C5	0	50	24	0	26
SS	C6	0	37	13	0	50
FS	D7	0	17	0	18	65
FS	D8	0	34	0	10	56
FS	D9	0	12	0	8	80
FS	E10	0	42	0	16	42

*Inclusion types per 100 inclusions; MHA: May-Hegglin anomaly; SS: Sebastian syndrome; FS: Fechtner syndrome; ECS: elongated ribosomic-banded cross-striated inclusions without endoplasmic reticulum segments; RA: ribosome aggregates without other structures.

along the long axis of the inclusion.

Classic FS/SS inclusions. The classic FS/SS Inclusions were round (about 0.9 – 1.3 µm in diameter) or oval (about 1.2 – 3.5×0.9 – 1.5 µm), and not enclosed by membranes. Most of them showed one or more segments of RER, preferentially in the periphery but sometimes in the matrix of the inclusion (Figure 3A). They contained single and clustered ribosomes and, sometimes, faint unorganized filaments.

FS/SS inclusions with cross-striated bands. These inclusions, which were about 1.5 – 3.5 µm long and 1.0 – 1.4 µm wide, looked like typical FS/SS inclusions but showed cross-striated bands of polyribosomes in their matrix (Figure 3B). The bands had a similar but more variable periodicity than the elongated-cross-striated inclusions described above.

Elongated cross-striated inclusions. These elongated

inclusions were generally spindle-shaped and about 2.2 to 7.1 µm in length and 0.3 to 0.6 µm in width (Figure 4). They were filled with clustered particles whose size (12 to 20 nm in diameter) and morphology were characteristic of ribosomes.²² These particles followed a cross-striated organization (about 290–350 nm in periodicity) and were accompanied by an amorphous background which was denser than the surrounding cytoplasm. Sporadically the inclusions showed a few segments of RER but not filaments. The elongated cross-striated inclusions could be located on the periphery of the nucleus, where they appeared slightly curved with the ribosome bands radially oriented (Figure 4A) or could be more elongated covering a long cytoplasmic area (Figure 4B).

Ribosome aggregates. Irregularly-shaped pure ribosome aggregates (ribosomes and/or polyribosomes) without strands of RER or filaments, measuring about 0.6 – 1.2 µm in diameter, were observed in all patients and healthy individuals (Figure 5), being much larger and abundant in the patients.

Other inclusion types. True Döhle bodies, made up of roughly parallel fragments of RER, were sporadically detected, and, in some cases, a number of pure SER inclusions were also observed.

Genetic studies

Within each family, the same mutation was identified in all affected members (Table 1). No mutations were detected in any unaffected individual.

Discussion

MYH9-related disorders with granulocyte inclusions are a group of autosomal dominant macrothrombocytopenias with a weak expression of bleeding diatheses, large platelets in blood smears, and Döhle-like inclu-

Table 3. MYH9-related disorders: follow-up results of 5 patients.

Diagnosis	Family-Case	*Platelet counts (×10 ⁹ /L)	Light microscopy: fraction of granulocytes with inclusions (%)	**Granulocyte ultrastructure: inclusion types (%)				
				FS/SS				
				MHA	classic	cross-striated	ECS	RA
MHA	A1 (1)	80	92	58	38	0	0	4
	(2)	95	97	73	23	0	0	4
SS	B4 (1)	94	61	0	30	36	0	34
	(2)	93	88	8	47	8	0	37
SS	C5 (1)	87	74	0	50	24	0	26
	(2)	64	35	18	31	28	0	23
FS	D7 (1)	154	46	0	17	0	18	65
	(2)	134	60	0	59	0	3	38
FS	D9 (1)	153	67	0	12	0	8	80
	(2)	181	80	0	76	0	5	19

*Microscopic platelet counts (normal range is 150 to 350); **Inclusion types per 100 inclusions; MHA: May-Hegglin anomaly; SS: Sebastian syndrome; FS: Fechtner syndrome; ECS: elongated ribosomic-banded cross-striated inclusions without endoplasmic reticulum segments; RA: ribosome aggregates without other structures; (1), (2): first, and second evaluation.

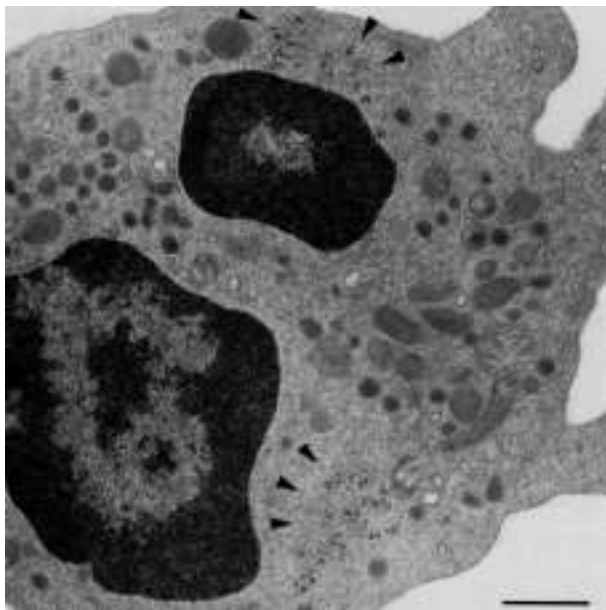


Figure 5. Ribosome aggregates. Electron micrograph of a neutrophil granulocyte showing two pure aggregates of ribosomes (arrowheads); bar = 1 μ m.

sions in granulocytes. These disorders include MHA, SS, which can be differentiated by subtle ultrastructural inclusion features, and FS, which includes associated clinical manifestations resembling the Alport syndrome: nephritis, high tone neurosensory deafness, and/or cataracts.^{21,23} Mutations in the *MYH9* gene, which encodes for the MHCIIA, have been reported in each of these syndromes and thus it can be agreed that all of these syndromes represent phenotypic variations of the same genetic anomaly.¹⁰

We studied granulocyte inclusions in a group of 10 patients from 5 unrelated families with MYH9-related disorders. As previously described, we found a wide range in the proportion of inclusions seen under light microscopy.²¹ This variation was also observed over time in some patients, though the predominant inclusion type remained constant (Table 3).

Ultrastructural evaluation of our patients' samples revealed a great variability in the number and morphology of granulocyte inclusions even among members of the same family (Table 2) and in the same patient over time (Table 3). The typical MHA inclusions (Figure 2) were found in significant amounts in both patients classified as having MHA. Moreover, these inclusions were identified in 2 % of cells in one SS patient (B3). Curiously, the other member of the same family (B4) showed 8 % of MHA inclusions in the second evaluation although these had not been observed in the first study. Another individual (C5), classified as having SS due to lack of MHA inclusions in the first study, also exhibited MHA inclusions in the second evaluation (18 %). On the

other hand, typical FS/SS inclusions were observed in variable amounts in all individuals, including those classified as having MHA (Table 2). Various technical aspects can influence granulocyte ultrastructure, such as sectioning: for example, a transverse plane of section of an MHA inclusion would appear as an FS/SS inclusion given that the cross sectioning would hide the longitudinal filaments. Variations in ultrastructure processing are additional causes of discrepancy. Despite these technical considerations, the morphologic variability observed was not sufficient to prevent the definition of a characteristic inclusion pattern in each patient.

The main type of inclusions found under electron microscopy in our SS and FS patients was the classic FS/SS inclusion (Figure 3A). We also observed similar inclusions presenting a cross-striated arrangement of ribosomes (Figure 3B). These inclusions are different from the SS compartmentalized inclusions reported by White *et al.*⁹ in which fragments of SER and glycogen particles produce segmentation. It cannot be ruled out that the different processing methodology, especially fixation, could account for the absence of these inclusions in our patients. However, the different processing cannot explain the lack of inclusions that have a sharp bend resembling the letter *L* in our samples.

All our FS patients also showed elongated spindle-shaped cross-striated inclusions, which have been previously observed in the perinuclear area.⁸ In the present study these inclusions were also detected in a wide cellular area in all parts of the cytoplasm (Figure 4).

A significant number of pure ribosome aggregates were identified in all the cases studied (Figure 5). To the best of our knowledge these have not been previously described in MYH9-related disorders. This observation could be related to the recently describe technique using MHCIIA immunocytochemistry.^{12,23,25} Employing this technique, the MHCIIA stain is diffusely distributed in the cytoplasm of normal granulocytes, whereas it makes up typical clusters in MYH9-related disorders. Using conventional stainings and light microscopy, the number of granulocyte inclusions observed is usually limited to one or two per cell whereas immunocytochemistry reveals a higher number of spots, including many small spots. Interestingly, the clustered MHCIIA is located within the basophil cytoplasmic inclusions that can be observed using conventional blood film staining. Moreover, the presence of ribosomes in the granulocyte inclusions had been previously established with the aid of the methyl-green-pyronin staining, and ultrastructural examinations.^{3,26} Although more specific studies (e.g. ultrastructural immunocytochemistry) should be performed to demonstrate this, the relevant number of ribosome aggregates and their spatial distribution resembling that of the MHCIIA clusters would suggest a relationship between

both structures.

Myosins are hexameric enzymes that convert ATP energy to mechanical work through their ATP-ase activity on actin. The type A non-muscle myosin is composed of two chains of MHCIIA and two distinct pairs of light chains.²⁷ Each heavy chain N terminus forms a globular head, complexed to a pair of light chains, which contain the actin- and ATP-binding sites. The C terminus, where the regulatory activity resides, forms an exclusive two-chain α -helical coiled-coil with a non-helical tailpiece on the end and is responsible for myosin filament polymerization. Several distinct mutations of the *MYH9* gene have been reported in hereditary macrothrombocytopenias, more frequently, involving the α -helical coiled-coil and tailpiece.¹⁰ Mutations in this site are thought to inhibit filament assembly leading to a failure in cytoskeletal reorganization.^{27,28} The head-myosin mutations generally correspond to MYH9-related disorders with Alport-like manifestations whereas those in the coiled-coil or tailpiece are more frequent in MHA and SS. The relative lack of correspondence between genetic mutations and phenotype as well as the wide phenotypic variations observed among members of the same family might be due to additional genetic factors,¹³ environmental influences, or stochastic variation. Our genetic studies revealed mutations in the *MYH9* gene, specifically the C terminal domain of MHCIIA, in all patients. Despite the limited number of cases, we observed a correlation between the genetic mutation and the phenotype. The E1841K mutation was associated with the MHA phenotype. Although this genetic anomaly has mainly been described in MHA patients it has also been described in some FS and Epstein cases.^{13,20,25,29,30} The nonsense R1933X mutation, which is known to produce a truncated C terminal MHCIIA, was detected in the individuals classified as having SS. Despite being reported in a few cases of SS, the R1933X mutation has more frequently been found in individuals with MHA.^{13,20,25,29-31} This mutation has also been identified in some FS individuals suffering from nephropathy as the sole Alport-like feature.^{13,32} In one of our FS families a mutation producing amino acid changes in position 1424 was detected (D1424Y). Although other mutations in this position have been mainly reported in FS, they have also been found in all types of MYH9 disorders.²³ The other FS family showed an R1165C mutation, previously described in FS, although this has also been found in SS.^{29,30}

Seri *et al.*³³ recently analyzed the genotype-phenotype correlations in a large number of patients with MYH9-related disorders. Interestingly, after an accurate clinical and laboratory evaluation, they found some Alport-like manifestations in a number of patients previously classified as having MHA or SS. In the light of these findings, it would be possible to infer an improvement in the genotype-phenotype correlation if the initial diagnoses (MHA, SS) were changed to FS. The mutations at the end of the myosin coiled-coil, especially at the most terminal exons, would be more frequently associated with MHA or SS. In contrast, the mutations in the region closer to the myosin head would be more frequently associated with Alport-like manifestations: FS and Epstein syndrome. Despite the small number of cases studied, our results follow the same tendency reflected in the aforementioned article. The mutations detected in the terminal region of the coiled-coil (exons 38 and 40) were observed in MHA and SS whereas those located in a region closer to the myosin head (exons 26 and 30) were observed in FS. As for the granulocyte inclusions, our results suggest that their ultrastructural characteristics could be associated with specific gene mutations: 1) the E1841K mutation with a high number of MHA inclusions, accompanied by a number of FS/SS inclusions, 2) the R1933X mutation with FS/SS inclusions including the classic and the cross-striated types, and 3) the R1165C, and D1424Y mutations with elongated cross-striated inclusions together with classic FS/SS. On the other hand, the presence of different inclusion types in the same patient, and even in the same cell, seem to confirm the close relationship among the MYH9-related disorders. It is reasonable to assume, therefore, that the ultrastructural morphology of the inclusions can be attributed to specific changes in the polymerization, assembly, or stability of the MHCIIA.

NPM and MJK were responsible for the design of the study, interpretation of the results and writing of the manuscript. NPM and AH performed the granulocyte ultrastructure and obtained the electron micrographs. MJK performed the MYH9 mutation analyses. EMD and IE contributed to the collection of data and interpretation of the results. All of the authors have approved the final version of the manuscript. We would like to thank Dr. Josep M. Salvadó (CAP Mollet, Barcelona, Spain) for referring one family for diagnosis and for permitting the use of the results for publication. The authors reported no potential conflicts of interest.

This work was supported in part by the NIH research grant 1R01HL66192 (to Michael J. Kelley) and by the Generalitat de Catalunya grant 2002XT-0032 (to Núria Pujol-Moix). Manuscript received July 25, 2003. Accepted December 3, 2003.

References

1. May R. Leukocyteneiscgüsse. *Deutsch Arch Klin Med* 1909;96:1-6.
2. Hegglin R. Gleichzeitige konstitutionelle Veränderungen and neutrophilen und thrombozyten. *Helvet Med Acta-Series A* 1945;4/5:439-40.
3. Jordan W, Larsen WE. Ultrastructural studies of the May-Hegglin anomaly. *Blood* 1965;25:921-32.
4. Peterson LC, Rao K, Crosson JT, White JG. Fechtner syndrome - A variant of Alport's syndrome with leukocyte inclusions and macrothrombocytopenia. *Blood* 1985; 65:397-406.
5. Rocca B, Laghi F, Zini G, Maggiano N, Landolfi R. Fechtner syndrome: report of a third family and literature review. *Br J Haematol* 1993;85:423-6.
6. Greinacher A, Nieuwenhuis HK, White JG. Sebastian platelet syndrome: a new variant of hereditary macrothrombocytopenia with leukocyte inclusions. *Blut* 1990; 61:282-8.

7. Pujol-Moix N, Muñiz-Diaz E, Moreno-Torres ML, Hernández A, Madoz P, Domingo A. Sebastian platelet syndrome. Two new cases in a Spanish family. *Ann Hematol* 1991;62:235-7.
8. Pujol-Moix N, Muñiz-Diaz E, Hernández A, Romero MA, Puig J. Fechtner syndrome variant: a new family with mild Alport's manifestations. *Br J Haematol* 1994; 86:686-7.
9. White JG, Mattson JC, Nichols WL, Luban NLC, Greinacher A. A variant of the Sebastian platelet syndrome with unique neutrophil inclusions. *Platelets* 2002; 13: 121-7.
10. OMIM*160775. Myosin, heavy chain 9, nonmuscle; MYH9. Online Mendelian Inheritance in Man. Available at URL: <http://www.ncbi.nlm.nih.gov/omim/>
11. Seri M, Savino M, Bordo D, Cusano R, Rocca B, Meloni I, et al. Epstein syndrome: another renal disorder with mutations in the nonmuscle myosin heavy chain 9 gene. *Hum Genet* 2002; 110: 182-6.
12. Pecci A, Noris P, Invernizzi R, Savoia A, Seri M, Ghiggeri GM, et al. Immunocytochemistry for the heavy chain of the non-muscle myosin IIA as a diagnostic tool for MYH9-related disorders. *Br J Haematol* 2002; 117:164-7.
13. Heath KE, Campos-Barros A, Toren A, Rozenfeld-Granot G, Carlsson LE, Savage J, et al. Nonmuscle myosin heavy chain IIA mutations define a spectrum of autosomal dominant macrothrombocytopenias: May-Hegglin anomaly and Fechtner, Sebastian, Epstein, and Alport-like syndromes. *Am J Hum Genet* 2001; 69: 1033-45.
14. Kashtan CE. Alport syndrome. An inherited disorder of renal, ocular, and cochlear basement membranes. *Medicine* 1999;78:338-60.
15. Maupin P, Phillips CL, Adelstein RS, Pollard TD. Differential localization of myosin-II isozymes in human cultured cells and blood cells. *J Cell Sci* 1994;107: 3077-90.
16. Pujol-Moix N, Muñiz-Diaz E, Hernández A, Durfort M. New types of granulocyte inclusions in hereditary macrothrombocytopenias. *Platelets* 2002;13:425-6.
17. Chanarin I. The blood count, its quality control and related methods. In: Chanarin I, ed. *Laboratory Haematology: an account of laboratory techniques*. Ciutat: Churchill Livingstone 1989:3-32.
18. Hotchkiss RD. A microchemical reaction resulting in the staining of polysaccharide structures in fixed tissue preparations. *Arch Biochem* 1948;16:131-41.
19. Heynen MJ, Blockmans D, Verwilghen RL, Vermeylen J. Congenital macrothrombocytopenia, leucocyte inclusions, deafness and proteinuria: functional and electron microscopic observations on platelets and megakaryocytes. *Br J Haematol* 1988; 70: 441-8.
20. Kelley MJ, Jawien W, Oertel TL, Korczak JF. Mutation of MYH9, encoding non-muscle myosin heavy chain 9, in May-Hegglin anomaly. *Nat Genet* 2000; 26: 106-8.
21. Greinacher A, Mueller-Eckhardt. Hereditary types of thrombocytopenia with giant platelets and inclusion bodies in the leukocytes. *Blut* 1990;60:53-60.
22. Ghadially FN. Endoplasmic reticulum. In: Ghadially FN, ed. *Ultrastructural pathology of the cell and matrix*, Volume 1 (3rd edition). Ciutat: Butterworths, 1988:413-571.
23. Balduini CL, Iolascon A, Savoia A. Inherited thrombocytopenias: from genes to therapy. *Haematologica* 2002;87:860-80.
24. Khalil SH, Qari MH. The Sebastian platelet syndrome. Report of the first native Saudi Arabian patient. *Pathology* 1995;27:197-8.
25. Kunishima S, Kojima T, Matsushita T, Tanaka T, Tsurusawa M, Furukawa Y, et al. Mutations in the NMMHC-A gene cause autosomal dominant macrothrombocytopenia with leukocyte inclusions (May-Hegglin anomaly/Sebastian syndrome). *Blood* 2001;97:1147-9.
26. Cawley JC, Hayhoe FGJ. The inclusions of the May-Hegglin anomaly and Döhle bodies of infection: an ultrastructural comparison. *Br J Haematol* 1972; 22:491-6.
27. Moores SL, Spudich JA. Conditional loss-of-myosin-II-function mutants reveal a position in the tail that is critical for filament nucleation. *Mol Cell* 1998; 1: 1043-50.
28. Deutsch S, Rideau A, Bochaton-Piallat ML, Merla G, Geinoz A, Gabbiani G, et al. Asp1424Asn MYH9 mutation results in an unstable protein responsible for the phenotypes in May-Hegglin anomaly/Fechtner syndrome. *Blood* 2003;102:529-34.
29. May-Hegglin/Fechtner Syndrome Consortium. Mutations in MYH9 result in the May-Hegglin anomaly, and Fechtner and Sebastian syndromes. *Nature Genet* 2000; 26:103-5.
30. Kunishima S, Matsushita T, Kojima T, Amemiya N, Choi YM, Hosaka N, et al. Identification of six novel MYH9 mutations and genotype-phenotype relationships in autosomal dominant macrothrombocytopenia with leukocyte inclusions. *J Hum Genet* 2001;46:722-9.
31. Martignetti JA, Heath KE, Harris J, Bizzaro N, Savoia A, Balduini CL, et al. The gene for May-Hegglin anomaly localizes to a less than 1-Mb region on chromosome 22q12.3-13.1. *Am J Hum Genet* 2000;66:1449-54.
32. Colville D, Wang YY, Jamieson R, Collins F, Hood J, Savage J. Absence of ocular manifestations in autosomal dominant Alport syndrome associated with haematological abnormalities. *Ophthalmic Genet* 2000;21:217-25.
33. Seri M, Pecci A, Di Bari F, Cusano R, Savino M, Panza E, et al. MYH9-related disease: May-Hegglin anomaly, Sebastian syndrome, Fechtner syndrome, and Epstein syndrome are not distinct entities but represent a variable expression of a single illness. *Medicine* 2003;82: 203-15.